water

MDPI

Article

New Interpretations of the Adsorption Process of Tetracycline on Biochar via Experimental and Theoretical Studies

Manel Ben Yahia [1,*] and Lotfi Sellaoui [2,*]

[1] Physics Department, Rabigh College of Science and Arts, King Abdulaziz University, Jeddah 21589, Saudi Arabia
[2] Laboratory of Quantum and Statistical Physics, Faculty of Sciences of Monastir, Monastir University, Monastir 5000, Tunisia
* Correspondence: mbinyhea@kau.edu.sa (M.B.Y.); sellaouilotfi@yahoo.fr (L.S.)

Abstract: A theoretical interpretation of the adsorption mechanism of tetracycline (TCCN) on biochar either in raw form (ADS1) or modified by chitosan-Fe/S (ADS2) is reported in the paper. An interpretative model is applied to the adsorption dataset, and considers that the adsorption of TCCN occurs with the formation of two layers on the investigated adsorbent. The theoretical model allows good data interpretation, confirming that TCCN adsorption capacity increases with temperature. The adsorption capacity at saturation (ACS) of TCCN on the ADS1 varied from 61.91 to 91.01 mg/g. while for ADS2 it varied from 135.76 to 202.50 mg/g. This difference is probably related to the difference in adsorbent properties and to the beneficial effect exerted by the adsorbent modification. Modeling results show also that TCCN is removed via a non-parallel orientation on both ADS1 and ADS2. For a thorough analysis of this mechanism, all adsorption energies (TCCN-ADS1, ADS2, and TCCN-TCCN) are determined at different temperatures.

Keywords: adsorption; tetracycline; biochar; modeling; sustainability of natural resources

check for updates

Citation: Yahia, M.B.; Sellaoui, L. New Interpretations of the Adsorption Process of Tetracycline on Biochar via Experimental and Theoretical Studies. *Water* **2022**, *14*, 3821. https://doi.org/10.3390/w14233821

Academic Editor: Zhiliang Zhu

Received: 21 October 2022
Accepted: 16 November 2022
Published: 23 November 2022

Publisher's Note: MDPI stays neutral with regard to jurisdictional claims in published maps and institutional affiliations.

Copyright: © 2022 by the authors. Licensee MDPI, Basel, Switzerland. This article is an open access article distributed under the terms and conditions of the Creative Commons Attribution (CC BY) license (https://creativecommons.org/licenses/by/4.0/).

1. Introduction

The presence of pharmaceutical compounds in the environment, such as tetracycline (TTCN), is responsible for increasing environmental pollution. The discharge of such products is principally related to the pharmaceutical industry and the use of veterinary and human medications [1–6]. Due to the wide application of this compound, it is considered as an emerging contaminant [7,8]. Although contaminated water is supposed to be treated by sewage treatment stations, their treatment capacity is not sufficient, and pharmaceuticals are not yet totally eliminated, hence direct discharge of residual TTCN is produced [9–11]. Therefore, it is necessary to apply a specific method to remove this pharmaceutical pollutant to protect the environment as well as human health. Literature indicates that there are different methods for removing TTCN and for reducing its concentration in water, such as membrane separation, adsorption, electrochemical degradation, and catalytic degradation [12–14]. Although all these methods are characterized by some advantages, the adsorption process is the most commonly applied in removing this pollutant, and appears to be the most attractive solution due to its high efficiency and easy manipulation [15]. For a better adsorptive removal of TTCN, the correct choice of adsorbent is the first step. In this context, different materials were employed to adsorb this compound and minimize its released concentration, such as biomaterials, carbon nanotubes, activated carbon, and graphene [16–20]. All these adsorbents showed a sufficient ability to remove this pollutant; however, their high cost urges the study of new affordable solutions. For instance, biochar is considered a promising adsorbent for removing this compound, as it is a multifunctional adsorbent able to treat various kinds of pollutants, to the point that it has become a hot research topic [21].

This research focused on the study of the adsorption of TTCN on biochar, either raw (ADS1) or modified by chitosan-Fe/S (ADS2), at different temperatures. Overall, the objective of this paper was to explain the TTCN adsorption mechanism via physical models, starting with the adsorption isotherms, and to describe the performance of the employed adsorbents. The application of physical models was adopted as a theoretical tool for attributing microscopic interpretations to the adsorption mechanism.

2. Experimental Adsorption Data: Batch Experiments

The adsorption data were retrieved at temperatures ranging between 298 and 318 K; to this aim, 50 mL conical flasks were filled with 25 mg of adsorbent and 25 mL of TCCN solution. The conical flasks were shaken in a thermodynamic water bath at 200 rpm. An ultraviolet-visible spectrometer (SHIMADZU, Japan) was used to determine the concentration of residual solution at 391 nm. The adsorption quantities were calculated with the corresponding equation for the material balance:

$$Q_e = \frac{V(C_0 - C_e)}{m} \quad (1)$$

C_0 and C_e are the initial and equilibrium concentrations of TTCN, m is adsorbent masse and V is the solution volume. Adsorption data and method of adsorbent preparation were illustrated according to this reference [22]. Figure 1 explains the variation in adsorption capacity as a function of equilibrium concentration in both systems.

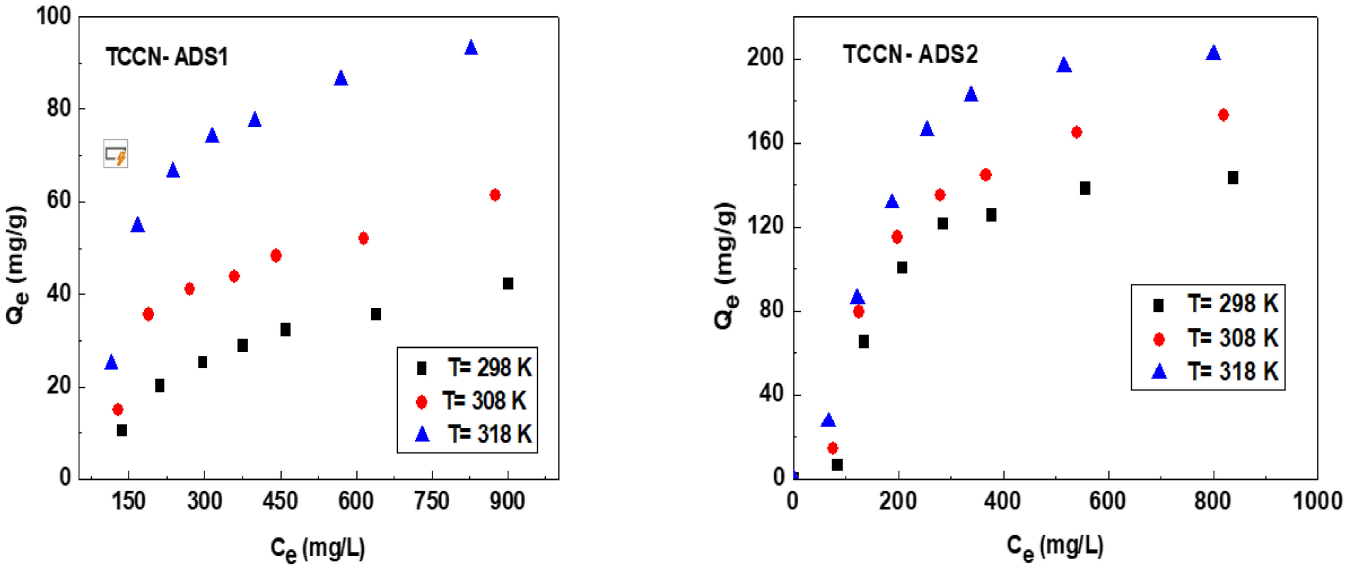


Figure 1. Adsorption data of TCCN on ADS1 and ADS2 at different temperatures.

According to Figure 1, it was noted that the ADS2 was characterized by high performance in removing the tested pollutant. In addition, an increment in the temperature led to an increment in the adsorption quantity of both investigated systems.

3. Theoretical Study

The modeling of adsorption experiments can be the first step to examining the adsorption mechanism. Based on the data in Figure 1, it is possible to deduce that the adsorption process can occur after the formation of one or more layers on the employed adsorbents. To simplify the modeling assessment at different temperatures, two advanced models were successfully adopted in the paper investigating whether the pollutant TCCN was removed by the formation of one (monolayer) and two layers (double layer).

3.1. Mono-Layer Adsorption Process: M1

Based on this model, the adsorption was considered as a monolayer process. In fact, one layer was formed on the employed adsorbents. Note that the interaction between the TCCN and the adsorbent surface was the result of layer formation. In addition, one adsorption functional group was the main agent responsible for TCCN molecules binding on adsorbent surface. In this situation, the expression of this model is summarized by [23].

$$Q_e = \frac{nD}{1 + \left(\frac{C_0}{C_e}\right)^n} \quad (2)$$

The adsorption process can be controlled via the model, in particular by their parameters: n is the estimated number of TCCN that is detected by each biochar active site, D is the receptor sites density, and C_0 is the concentration at half-saturation.

3.2. Double-Layer Adsorption Process: M2

This situation considered that two layers were formed on the adsorbent surface. Two adsorption energies were mainly responsible for this process. The first energy described the interactions between TCCN and the biochar surface, and the second described those between the TCCN molecules. The expression of this second model is mathematically described by [23]:

$$Q_e = nD_{RS}\frac{\left(\frac{C_e}{C_{01}}\right)^n + 2\left(\frac{C_e}{C_{02}}\right)^{2n}}{1 + \left(\frac{C_e}{C_{01}}\right)^n + \left(\frac{C_e}{C_{02}}\right)^{2n}} \quad (3)$$

Similarly to the previous model, in this case the adsorption mechanism can be analyzed by the interpretation of the model parameters: n is the estimated number of TCCN that was detected by the biochar active site, D_{RS} is the receptor site density, and C_{01} and C_{02} are the concentrations at half-saturation. These models were applied on the adsorption data depicted in Figure 1, and the fitting results showed that the second model was the best one to interpret the TTCN adsorption mechanism. The fitting of adsorption data indicated that there was no significant difference between the values of determination coefficient R^2 of the tested models, but the impact of temperature on the parameters of second model was more meaningful, as more plausible insights in the TCCN adsorption mechanism could be retrieved. In summary, the determined values of the double layer model (M2), which was the most adequate for data description, are listed in Table 1. Examples of the fitting of TCCN adsorption data are reported in the Appendix A.

Table 1. Double layer (M2) model parameters as a function of temperature (T = 298, 308 and 318 K).

	n	D_{RS} (mg/g)	Q_{ACS} (mg/g)	E_1 (kJ/mol)	E_2 (kJ/mol)
			TCCN-ADS1		
298 K	2.63	11.77	61.91	6.88	5.14
308 K	1.79	19.08	68.30	10.19	8.84
318 K	1.90	23.95	91	13.44	9.87
			TCCN-ADS2		
298 K	6.61	10.27	135.76	7.79	7.22
308 K	3.56	23.64	168.31	11.32	9.14
318 K	3.28	30.87	202.5	14.54	10.98

4. Assessment of TCCN Adsorption Mechanism

4.1. Interpretation of ACS

Based on the application of the selected model, the TCCN adsorption mechanism was analyzed. At high TCCN equilibrium concentration, the adsorption capacity at saturation (ACS) could be estimated. In this situation, the ACS expression is: $2.n.\ D_{RS}$. To analyze

the impact of temperature on this ACS (see Figure 2), it is clear that the temperature had a positive effect. In particular, the temperature increase led to an increase in the ACS of both the adsorbents. Clearly, the temperature plays a positive role in removing this pharmaceutical compound. At all temperatures, the comparison of the ACS followed this sequence: Q_{ACS} (TCCN- ADS1) > Q_{ACS} (TCCN- ADS2). Note that the ACS of TCCN on the ADS1 varied from 61.91 to 91.01 mg/g, while the ACS of TCCN on the ADS2 varied from 135.76 to 202.50 mg/g. This difference was probably related to the difference in adsorbent properties, such as surface area and chemical composition, due to the surface modification. For industrial application, the ADS2 can be suggested as proficient, even if it requires some surface modification for better adsorptive removal of this pharmaceutical.

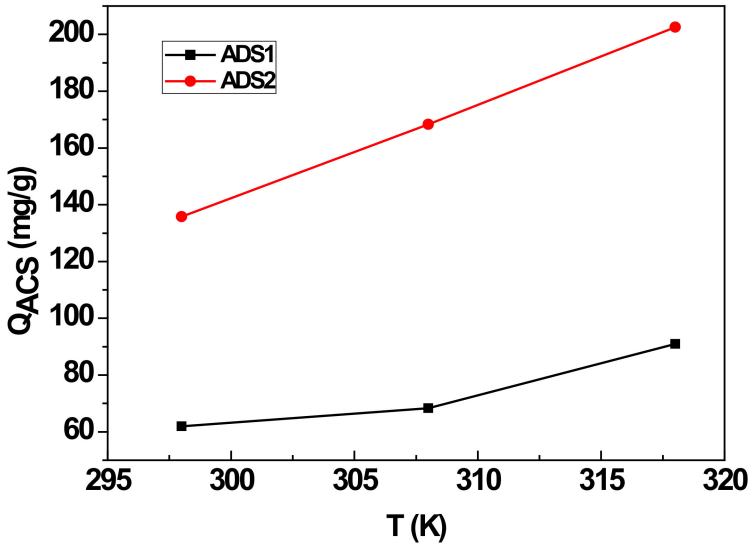


Figure 2. Impact of temperature on ACS of TTCCN for both the adsorbents.

4.2. Estimated Number of TCCN That is Detected by Biochar Adsorption Site (n)

Overall, the investigation of this parameter can supply different insights in the physicochemical aspects of the adsorption mechanism. Note that the values decreased from 2.63 to 1.90 and from 6.61 to 3.28 in the systems TCCN-ADS1 and TCCN-ADS2, respectively. These determined values indicated that the TCCN compound was aggregated during the adsorption process, but the aggregation degree is different from one system to another, and also differs according to the temperature. For instance, the TCCN practically formed a dimer for the system TCCN-ADS1 at T = 318 K (n = 1.9), while for the system TCCN-ADS2, a trimer was formed at the same temperature. Since the number of TCCN detected per adsorption site decreased with temperature, we can understand that the aggregation degree also decreased as a function of temperature. In conclusion, both adsorption systems were thermally activated, and activation energy was the main factor for the aggregation formation. Notably, it is clear that: n (TCCN-ADS2) > n (TCCN-ADS1). This theoretical result proved that the modification of the adsorbent surface increased the affinity of active sites to capture more TCCN molecules. The parameter can also provide important indications about the TCCN orientation on both the adsorbents (Figure A1). To describe the TCCN orientation, the possible cases are summarized in Table 2.

The results of adsorption data fitting listed in Table 1 showed that all the calculated values of this parameter were superior to the unity. Certainly, it is clear that the TCCN was removed by a single interaction with the adsorbent surface. Thus, this compound was adsorbed via a non-parallel orientation.

Figure 3 illustrates the impact of temperature on the estimated number of TCCN detected by biochar active site. Referring to this Figure, it is notable that the increment in temperature resulted in a decrease in this parameter, which was probably due to the increase in thermal agitation.

Table 2. Possible cases to describe the TCCN orientation on both adsorbents.

Possible Cases	Type of Orientation
If $n \leq 0.5$	Parallel orientation: the TCCN can be removed via an interaction with two sites
If $n < 0.5 < 1$	Parallel and non-parallel orientation at the same time
$n > 1$	Non-parallel orientation: the TCCN can be removed via an interaction with one site

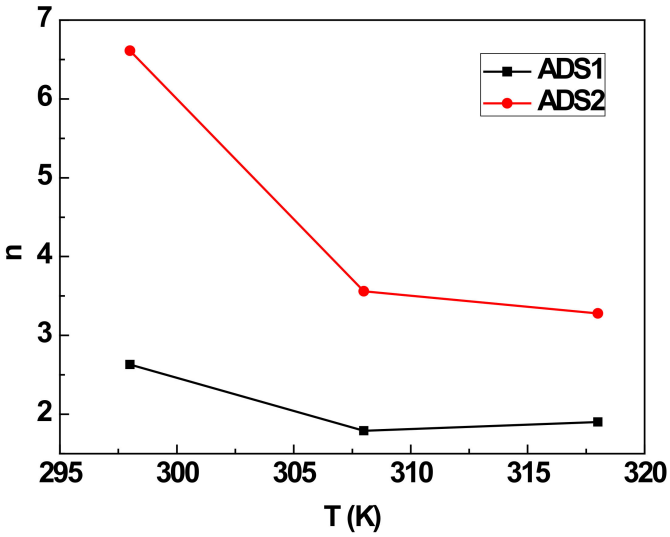


Figure 3. Impact of temperature on the parameter n.

4.3. Parameter D_{RS}

For both the adsorption systems, it is clear that the adsorption density increased with temperature (Figure 4). This behavior can be explained by various factors. First, an increment of this density is probably due to the appearance of additional active adsorption sites that can participate in removing the TCCN compound. Secondly, this increment can be also explained by the decrement in the number of TCCN molecules detected by the adsorption site. In particular, a decrement in this number of molecules per site can provide more space on both employed adsorbents, leading to an increment in this adsorption density.

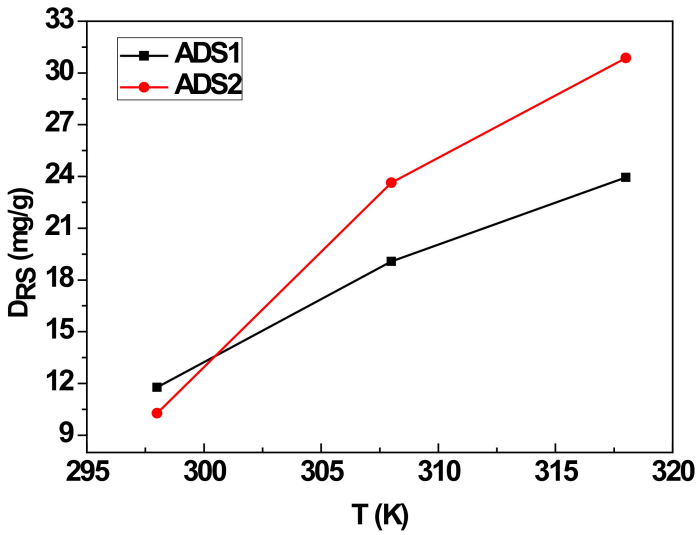


Figure 4. Impact of temperature on the parameter D_{RS}.

5. Adsorption Energy and General Discussion

The adsorption energies that characterize the interactions between TCCN and either ADS1 or ADS2 (E_1), and among TCCN molecules (E_1) were calculated through the following expressions (the values are listed in Table 1):

$$E_1 = \text{RT.log}\ (s/c_{01}) \quad (4)$$

$$E_2 = \text{RT.log}\ (s/c_{02}) \quad (5)$$

In these expressions, s represents the TCCN solubility, R is the ideal gas constant (R = 8.314 J. mol^{-1}, and K^{-1}) is the TCCN water solubility. Based on the estimated values of both the adsorption energies, it is possible to conclude that the adsorption of TCCN was achieved by physical interactions via an endothermic process. Figure 5 illustrates the effect of temperature on adsorption energies, allowing visualization of its increment. This fact is reasonably explained by the positive effect of temperature on ACS.

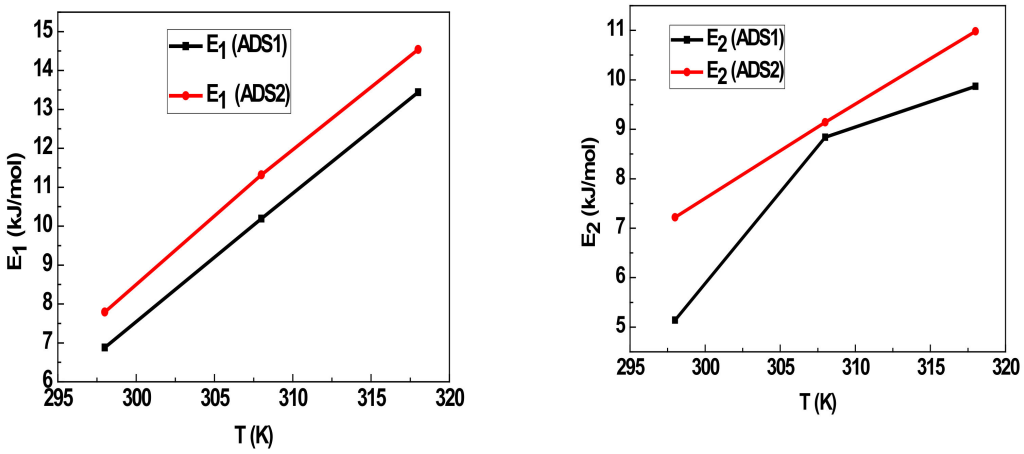


Figure 5. Trend of adsorption energies as a function of temperature.

Referring to our interpretations, we demonstrated that Q_{ACS} (TCCN-ADS1) > Q_{ACS} (TCCN-ADS2). In the same direction, it was found that: n (TCCN-ADS2) > n (TCCN-ADS1). Based on these comparisons, we can conclude that the ACS was controlled by the parameter n. Additionally, it was found that: E_1 (TCCN-ADS2) > E_1 (TCCN-ADS1) and E_2 (TCCN-ADS2) > E_2 (TCCN-ADS1). All these findings showed that the TCCN adsorption mechanism was governed by the adsorption energies and the number of detected molecules per biochar adsorbent site.

6. Conclusions

In this research, biochar, both in raw form (ADS1) and modified by chitosan-Fe/S (ADS2), was investigated to interpret the adsorption isotherms of tetracycline (TCCN). Based on theoretical evidence, it was noted that the modification of the adsorbent surface ameliorated its performance, which is useful for real industrial applications. An aggregation process among TCCN molecules was identified upon adsorption, but its degree differs from one system to another and also according to the temperature. The TCCN was removed via a non-parallel orientation on an adsorbent surface. The estimated adsorption energies suggested that the TCCN was removed via physical interactions on both the adsorbents, and its adsorption process is endothermic. Overall, this theoretical mechanism was controlled by the adsorption energies and by the number of detected molecules per biochar active site.

Author Contributions: Conceptualization, M.B.Y.; methodology, L.S.; software, M.B.Y.; validation, L.S., M.B.Y. and L.S.; formal analysis, L.S. Investigation, M.B.Y.; resources, M.B.Y.; data curation, L.S.; writing—original draft preparation, M.B.Y.; writing—review and editing, L.S.; visualization, L.S.; supervision, M.B.Y.; project administration, M.B.Y.; funding acquisition, M.B.Y. All authors have read and agreed to the published version of the manuscript.

Funding: The Deanship of Scientific Research (DSR) at King Abdulaziz University (KAU), Jeddah, Saudi Arabia funded this Project under grant no. (G: 460-665-1443).

Institutional Review Board Statement: Not applicable.

Informed Consent Statement: Not applicable.

Data Availability Statement: Not applicable.

Conflicts of Interest: The authors declare no conflict of interest.

Appendix A

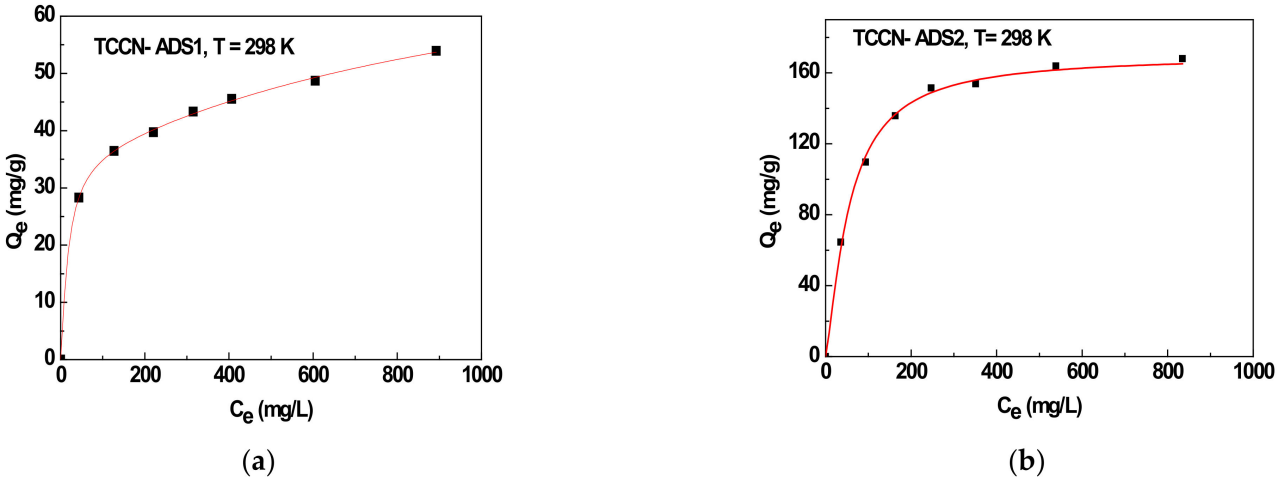


Figure A1. Examples of adsorption data fitting; (**a**) TCCN-ADS1 (**b**) TCCN-ADS2.

References

1. Le-Minh, N.; Khan, S.J.; Drewes, J.E.; Stuetz, R.M. Fate of antibiotics during municipal water recycling treatment processes. *Water Res.* **2010**, *44*, 4295–4323. [CrossRef]
2. Fuoco, D. Classification Framework and Chemical Biology of Tetracycline-Structure-Based Drugs. *Antibiotics* **2012**, *1*, 1–13. [CrossRef]
3. Omidvar, M.; Mousavi, S.M.; Soltanieh, M.; Safekordi, A.A. Preparation and characterization of poly (ethersulfone) nanofiltration membranes for amoxicillin removal from contaminated water. *J. Environ. Health Sci. Eng.* **2014**, *12*, 18. [CrossRef]
4. Chen, J.; Zhang, D.; Zhang, H.; Ghosh, S.; Pan, B. Fast and slow adsorption of carbamazepine on biochar as affected by carbon structure and mineral composition. *Sci. Total Environ.* **2017**, *579*, 598–605. [CrossRef]
5. Norvill, Z.N.; Toledo-Cervantes, A.; Blanco, S.; Shilton, A.; Guieysse, B.; Muñoz, R. Photodegradation and sorption govern tetracycline removal during wastewater treatment in algal ponds. *Bioresour. Technol.* **2017**, *232*, 35–43. [CrossRef]
6. Liu, H.-Q.; Lam, J.C.; Li, W.-W.; Yu, H.-Q.; Lam, P.K. Spatial distribution and removal performance of pharmaceuticals in municipal wastewater treatment plants in China. *Sci. Total Environ.* **2017**, *586*, 1162–1169. [CrossRef]
7. Baumgarten, B.; Jährig, J.; Reemtsma, T.; Jekel, M. Long term laboratory column experiments to simulate bank filtration: Factors controlling removal of sulfamethoxazole. *Water Res.* **2011**, *45*, 211–220. [CrossRef]
8. Homem, V.; Santos, L. Degradation and removal methods of antibiotics from aqueous matrices—A review. *J. Environ. Manag.* **2011**, *92*, 2304–2347. [CrossRef]
9. Gao, L.; Sun, Y.; He, L.; Zhao, W.; Xiang, G.; Jiang, X.; Zhang, S. A polyhedral oligomeric silsesquioxanes/dual ligands-based magnetic adsorbent for effective extraction of aflatoxins in cereals via multiple interactions. *Microchem. J.* **2021**, *160*, 105626. [CrossRef]
10. Leung, H.; Minh, T.; Murphy, M.; Lam, J.C.; So, M.; Martin, M.; Lam, P.K.; Richardson, B. Distribution, fate and risk assessment of antibiotics in sewage treatment plants in Hong Kong, South China. *Environ. Int.* **2012**, *42*, 1–9. [CrossRef]
11. Xu, J.; Xu, Y.; Wang, H.; Guo, C.; Qiu, H.; He, Y.; Zhang, Y.; Li, X.; Meng, W. Occurrence of antibiotics and antibiotic resistance genes in a sewage treatment plant and its effluent-receiving river. *Chemosphere* **2015**, *119*, 1379–1385. [CrossRef]

12. Lu, T.; Xu, X.; Liu, X.; Sun, T. Super hydrophilic PVDF based composite membrane for efficient separation of tetracycline. *Chem. Eng. J.* **2017**, *308*, 151–159. [CrossRef]
13. Yang, S.; Feng, Y.; Gao, D.; Wang, X.; Suo, N.; Yu, Y.; Zhang, S. Electrocatalysis degradation of tetracycline in a three-dimensional aeration electrocatalysis reactor (3D-AER) with a flotation-tailings particle electrode (FPE): Physicochemical properties, influencing factors and the degradation mechanism. *J. Hazard. Mater.* **2021**, *407*, 124361. [CrossRef]
14. Chen, B.; Li, Y.; Li, M.; Cui, M.; Xu, W.; Li, L.; Sun, Y.; Wang, M.; Zhang, Y.; Chen, K. Rapid adsorption of tetracycline in aqueous solution by using MOF-525/graphene oxide composite. *Microporous Mesoporous Mater.* **2021**, *328*, 111457. [CrossRef]
15. Pandi, K.; Choi, J. Selective removal of anionic ions from aqueous environment using iron-based metal-organic frameworks and their mechanistic investigations. *J. Mol. Liq.* **2021**, *329*, 115367. [CrossRef]
16. Huang, D.; Wu, J.; Wang, L.; Liu, X.; Meng, J.; Tang, X.; Tang, C.; Xu, J. Novel insight into adsorption and co-adsorption of heavy metal ions and an organic pollutant by magnetic graphene nanomaterials in water. *Chem. Eng. J.* **2019**, *358*, 1399–1409. [CrossRef]
17. Bai, Y.; Su, J.; Wen, Q.; Li, G.; Xue, L.; Huang, T. Removal of tetracycline by denitrifying Mn (II)-oxidizing bacterium *Pseudomonas* sp. H117 and biomaterials (BMO and MBMO): Efficiency and mechanisms. *Bioresour. Technol.* **2020**, *312*, 123565. [CrossRef]
18. Duan, Z.; Zhang, W.; Lu, M.; Shao, Z.; Huang, W.; Li, J.; Li, Y.; Mo, J.; Li, Y.; Chen, C. Magnetic Fe3O4/activated carbon for combined adsorption and Fenton oxidation of 4-chlorophenol. *Carbon* **2020**, *167*, 351–363. [CrossRef]
19. Zaher, A.; Taha, M.; Mahmoud, R.K. Possible adsorption mechanisms of the removal of tetracycline from water by La-doped Zn-Fe-layered double hydroxide. *J. Mol. Liq.* **2021**, *322*, 114546. [CrossRef]
20. Zhao, W.; Tian, Y.; Chu, X.; Cui, L.; Zhang, H.; Li, M.; Zhao, P. Preparation and characteristics of a magnetic carbon nanotube adsorbent: Its efficient adsorption and recoverable performances. *Sep. Purif. Technol.* **2021**, *257*, 117917. [CrossRef]
21. Xiang, W.; Zhang, X.; Chen, J.; Zou, W.; He, F.; Hu, X.; Tsang, D.C.W.; Ok, Y.S.; Gao, B. Biochar technology in wastewater treatment: A critical review. *Chemosphere* **2020**, *252*, 126539. [CrossRef]
22. Liu, J.; Zhou, B.; Zhang, H.; Ma, J.; Mu, B.; Zhang, W. A novel Biochar modified by Chitosan-Fe/S for tetracycline adsorption and studies on site energy distribution. *Bioresour. Technol.* **2019**, *294*, 122152. [CrossRef]
23. Sellaoui, L.; Guedidi, H.; Knani, S.; Reinert, L.; Duclaux, L.; Ben Lamine, A. Application of statistical physics formalism to the modeling of adsorption isotherms of ibuprofen on activated carbon. *Fluid Phase Equilibria* **2015**, *387*, 103–110. [CrossRef]